Inorganic Chemistry

Article

pubs.acs.org/IC

Novel Refractory Phase, $Ta_7Si_2(Si_xB_{1-x})_2$

V. Romaka,[†,#] V. Fosodeder,[†] P. F. Rogl,*[,†] É. C. T. Ramos,[‡] C. A. Nunes,[§] G. C. Coelho,[§,∥] and G. Giester[⊥]

[†]Institute of Physical Chemistry, University of Vienna, Währingerstrasse 42, A-1090 Wien, Austria

[‡]Universidade Federal de Alfenas, Cidade Universitária, Rodovia José Aurélio Vilela 11999, 37715-400 Poços de Caldas, Minas Gerais, Brazil

[§]Departamento de Engenharia de Materiais (DEMAR), Escola de Engenharia de Lorena (EEL), Universidade de São Paulo (USP), Polo Urbo-Industrial Gleba AI-6 s/n, 12600-000 Lorena, São Paulo, Brazil

[∥]Mestrado Profissional em Materiais, Centro Universitário de Volta Redonda, Av. Paulo Erlei Alves Abrantes 1325, 27240-560 Volta Redonda, Rio de Janeiro, Brazil

[⊥]Institute of Mineralogy and Crystallography, University of Vienna, Althanstrasse14, A-1090 Wien, Austria

Supporting Information

ABSTRACT: X-ray single crystal (XSC) and powder diffraction data (XPD) were used to elucidate the crystal structure of a new refractory silicon boride $Ta_7Si_2(Si_xB_{1-x})_2$ (x = 0.12). Tetragonal $Ta_7Si_2(Si_xB_{1-x})_2$ (space group $P4/mbm$; a = 0.62219(2) nm, c = 0.83283(3) nm) with B atoms randomly sharing the 4g site with Si atoms is isotypic with the boride structure of $(Re,Co)_7B_4$. The architecture of the structure of $Ta_7Si_2(Si_xB_{1-x})_2$ combines layers of three-capped triangular metal prisms (Si,B)[Ta_{6+2}(Si,B)] alternating with double layers of two-capped Si[Ta_{8+1}Si] Archimedian metal antiprisms. Consequently, the metal framework contains (B/Si) pairs and Si−Si dumbbells. These two types of coordination figures around the nonmetal atoms are typical for the system-inherent structures of Ta_2B (or Ta_2Si) and Ta_3B_2. DFT calculations showed strong B(Si)−B(Si) and Si−Si bonding and represent $Ta_7Si_2(Si_xB_{1-x})_2$ as a covalent−ionic compound. This bonding behavior is reflected in the high hardness value of 1750 HV. The Sommerfeld constant, γ = 7.58 mJ/mol K^2, as derived from the electronic density of states, calculated at the Fermi level, suggests typical metallic behavior.

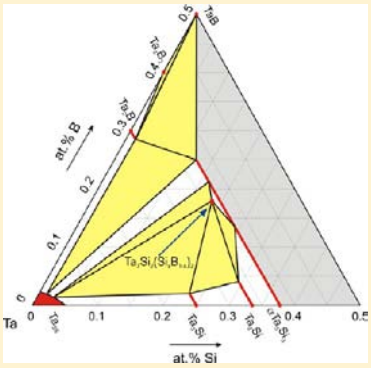

1. INTRODUCTION

At high temperatures, silicon borides of refractory transition metals (TM) and in particular the solid solution phases with stoichiometry $(TM1,TM2)_5(Si,B)_3$ exhibit good oxidation resistance, high yield stress and compressive strength, and good creep resistance and thus qualify as promising materials for high-temperature applications.[1−3] In some TM−Si−B systems, the $(TM)_5(Si,B)_3$ phases are found in equilibrium with the parent metal matrix in the form of a disperse eutectic structure (in situ metal−matrix composite), providing a good base for the development of high-temperature structural materials.[2,3]

Tantalum is one of the most refractory metals as well as some of its compounds with B, C, and N. Because of the high hardness of these materials, sputtered $Ta_xSi_yB_z$ substrates, for instance, provide inkjet printer heads suitable for high-speed recording.[4] Early reports on the constitution of the Ta−Si−B system identified two ternary phases.[5,6] Both phases were described as deriving from the stoichiometry Ta_5Si_3 and were labeled as $D8_8$ (Mn_5Si_3-type, stabilized by the incorporation of B into the Ta_5Si_3 structure) and as T2 (Cr_5B_3-type), the latter of which has a composition close to the Ta−Si boundary stabilized by substitutional Si/B exchange $Ta_5(Si,B)_3$.[5,6] It should be noted here that according to the latest assessment of the Ta−Si phase diagram,[7] Ta_5Si_3 exhibits two structure modifications. The high-temperature form βTa_5Si_3 (W_5Si_3-type; mp 2533 °C) transforms at 2160 °C into the low-temperature modification αTa_5Si_3 with the Cr_5B_3-type. Later attempts to derive the phase relations in the Ta-rich region of the Ta−Si−B system at 1900 °C (arc-melted alloys annealed at 1900 °C for 48 h) (a) confirmed the T2 phase with a continuous phase region extending from binary αTa_5Si_3 to $Ta_5(Si_{1-x}B_x)_3$, x = 0.70 and (b) observed a new phase ϕ with unknown structure type, which was tentatively located at the composition $Ta_2(Si_{0.54}B_{0.46})$.[8] Ball-milling of powders Ta-12.5 atom % Si-25 atom % B yielded an amorphous phase after 200 h, which on reheating at 1200 °C for 4 h recrystallized to a phase mixture of T2 + TaB, revealing in addition a (further?) unknown phase.[9] More recent attempts to shed light on the structural chemistry of {Nb,Ta}−Si−B phases from X-ray single-crystal data dealt with the crystal structures of $Ta_3(Si_{0.89}B_{0.11})$, which crystallizes with the Ti_3P-type, where B and Si atoms randomly share the 8g site, and $Ta_5(Si_{0.43}B_{0.57})_3$ for which the Cr_5B_3-type has been confirmed, where B atoms replace Si on the 8h site.[10] These cases demonstrate

Received: June 19, 2013
Published: September 19, 2013

Table 1. X-ray Single Crystal Data for $Ta_7Si_2(Si_xB_{1-x})_2$, $x = 0.12$[a]

parameter	$Ta_7Si_2(Si_{0.12}B_{0.88})_2$
structure type	$Ta_7Si_2(Si_xB_{1-x})_2$
composition from EPMA	$Ta_{63.6}Si_{18.5}B_{17.9}$
composition from refinement	$Ta_{63.6}Si_{20.4}B_{16}$
formula from refinement	$Ta_7Si_2(Si_xB_{1-x})_2$; $x = 0.12$
space group	*P4/mbm* (no. 127)
a, *c* (nm) single crystal data	0.62219(2), 0.83283(3)
a, *c* (nm)[b]	0.62048(2), 0.83136(9)
crystal size (μm)	20 × 25 × 35
μ_{abs} (mm^{-1})	118.55
ρ_x (g cm^{-3})	13.89
reflections in refinement	422 ≥ 4σ (F_o) of 437
mosaicity	0.56
number of variables	19
$R_F = \Sigma\|F_o - F_c\|/\Sigma F_o$	0.0237
R_{int}	0.067
wR2	0.0485
GOF	1.308
extinction (Zachariasen)	0.0013(1)
residual density ($e^-/Å^3$); max; min	3.5; −3.66
Ta1 in 8k (*x*, *x*+1/2, *z*); *x*, *z*	0.66794(4); 0.19719(4)
occ.	1.0
U_{11}=U_{22}; U_{33}; U_{23}=U_{13}; U_{12}	0.0033(1); 0.0023(2); −0.0003(0); 0.0008(1)
Ta2 in 4h (*x*, *x*+1/2, 1/2); *x*	0.15948(6)
occ.	1.0
U_{11}=U_{22}; U_{33}; U_{12}	0.0033(1); 0.0012(2); −0.0002(2)
M1 in 4g (x, x+1/2, 0); x	0.1196(13)
occ.	0.88 B1 + 0.12(1) Si1
$U_{iso} = U_{eq}$	0.0050(17)
Si2 in 4e (0, 0, *z*); *z*	0.3423(4)
occ.	1.0
U_{11}=U_{22}; U_{33}	0.0029(8); 0.0036(13)
Ta3 in 2a (0, 0, 0)	
occ.	1.0
U_{11}= U_{22}; U_{33}	0.0025(2); 0.0014(2)
	principal axes (U_{ii}', U_{eq}) of ADP ellipsoids
Ta1	0.0042 0.0026 0.0021 0.0030(1)
Ta2	0.0035 0.0031 0.0012 0.0026(1)
Si2	0.0036 0.0028 0.0028 0.0031(6)
Ta3	0.0025 0.0025 0.0014 0.0021(1)

interatomic distances (nm) for $Ta_7Si_2(Si_xB_{1-x})_2$[c]

Ta1 (CN = 16)	2 B1/Si1	0.24470
	B1/Si1	0.24885
	2 Si2	0.26118
	2 Ta3	0.28386
	Ta2	0.29438
	Ta1	0.29554
	2 Ta2	0.32423
	4 Ta1	0.32743
	Ta1	0.32845
Ta2 (CN = 15)	4 Si2	0.26828
	Ta2	0.28066
	2 Ta1	0.29438
	4 Ta1	0.32423
	4 Ta2	0.33086
B1/Si1 (CN = 9)	B1/Si1	0.21044
	4 Ta1	0.24470
	2 Ta3	0.24811
	2 Ta1	0.24885
Si2 (CN = 10)	4 Ta1	0.26118
	Si2	0.26261
	4 Ta2	0.26828
	Ta3	0.28511
Ta3 (CN = 14)	4 B1/Si1	0.24811
	8 Ta1	0.28386
	2 Si2	0.28511

[a]Standardized with the program Structure Tidy.[27] Data collection details: Mo Kα radiation; 2 < 2θ < 71.96°; ω-scans, scan width 2°; 250 s/frame, 460 frames, 9 sets, redundancy >9. Anisotropic displacement parameters U_{ij} and U_{iso} (in 10^{-2} nm^2). [b]Guinier−Huber X-ray powder data employing Ge as the standard. [c] Standard deviations ≤0.0002 nm.

a strong stabilizing effect of boron incorporation in the Ta-silicides investigated.

Therefore, the aim of the present article is the determination of the crystal structure of the unknown phase ϕ, which hitherto was tentatively located at the composition $Ta_2(Si_{0.54}B_{0.46})$.[8] The details of the atom site occupation will provide the basis for (a) a proper phase triangulation of the isothermal Ta−Si−B sections, (b) for a proper definition of the thermodynamic stability, and (c) the sublattice model in a future thermodynamic modeling of the constitution of the ternary system Ta−Si−B.

2. EXPERIMENTAL SECTION

Alloys were prepared from metal ingots of Ta (min. 99.5 mass %), Si (min. 99.998%), and B (min. 99.5 mass %) by repeated arc melting under argon (weight loss of less than 0.1%). The reguli were then annealed in a W-mesh heated furnace under argon at 2000 °C for 100 h or at 2300 °C for 45 h followed by furnace cooling. Lattice parameters and standard deviations were determined by least-squares refinements of room temperature X-ray powder diffraction (XRD) data obtained from a Guinier−Huber image plate employing monochromatic Cu Kα_1 radiation and Ge as the internal standard (a_{Ge} = 0.565791 nm). XRD-Rietveld refinements were performed with the FULLPROF program[11] with the use of its internal tables for atom scattering factors. The annealed samples were polished using standard procedures and were examined by scanning electron microscopy (SEM). Quantitative compositions were determined on a CAMEBAX SX-50 electron-beam probe microanalyzer (WDX) with an electron beam current of 15 nA. Pure elements served as standards to carry out the deconvolution of overlapping peaks and background subtraction. Finally, the X-ray intensities were corrected for ZAF effects using the INCA-Energy 300 software package.[12] The overall composition of the samples derived from EPMA area scans agree with the nominal values within 1.0 atom %.

Single crystals of $Ta_7(Si_{1-x}B_x)_4$ were isolated via mechanical fragmentation of a specimen with nominal composition $Ta_{64.0}Si_{20.0}B_{16.0}$, which has been annealed for 45 h at 2300 °C. X-ray single crystal (XSC) intensity data were collected on a four-circle Nonius Kappa diffractometer (CCD area detector and graphite monochromated Mo Kα radiation, λ = 0.071069 nm). Orientation matrix and unit cell parameters were derived using the program DENZO.[13] No individual absorption correction was necessary because of the rather regular crystal shape and small dimensions of the investigated specimens. The structures were solved by direct methods and refined with the SHELXS-97 and SHELXL-97 programs,[14] respectively. Further details concerning the experiments are summarized in Table 1. Using the DIDODATA program,[15] we derived the Voronoi coordination polyhedra for all atom sites in the compounds investigated.

Hardness measurements of the new phase were carried out using a Buehler Micromet2004 microhardness tester with 300 gf load and 30 s indentation time.

dx.doi.org/10.1021/ic401413f | Inorg. Chem. 2013, 52, 11295−11301

DFT (density functional theory) electronic structure calculations for $Ta_7(Si_{1-x}B_x)_4$ (x = 0.44) (with experimentally determined structural parameters) were carried out with the Elk package[16] (an all-electron full-potential linearized augmented-plane wave code with PBE parametrization[17]). VESTA[18] was used for crystal structure and volumetric data visualization of the electron localization function (ELF).

3. RESULTS AND DISCUSSION

3.1. Determination of the Crystal Structure of $Ta_7Si_2(Si_xB_{1-x})_2$ (x = 0.12). Analyses of the X-ray single crystal data set, particularly the systematic extinctions (observed for $0kl$, k = 2n + 1 and $h00$ for h = 2n + 1), prompted a primitive tetragonal unit cell (a = 0.62219(2) nm and c = 0.83283(3) nm) consistent with space group symmetries $P4/mbm$ (no. 127), $P\bar{4}b2$ (no. 117), and $P4bm$ (no. 100), out of which the highest symmetric one, $P4/mbm$, was chosen for further structure analysis. Direct methods delivered a structure solution with three sites for Ta atoms: one site consistent with a full occupation by Si atoms and another site with a considerably smaller electron density. Refinement with isotropic atom-displacement parameters (ADPs) clearly indicated boron atoms in the latter position, although as a mixed position with Si atoms to avoid an unusually low ADP parameter for this site. Introducing a free variable for the mixed Si/B occupation resulted in 0.88 B + 0.12(1) Si. A final refinement inferring anisotropic atom-displacement parameters in general but isotropic ADPs for the mixed site converged to a value R_F = 0.0237 with density Fourier ripples of less than 3.5 $e^-/Å^3$ at 0.01 nm from Ta3. An analysis of the missing symmetry by program PLATON (within the Windows version WINGX[19]) confirmed the space group chosen: $P4/mbm$. The parameters used for refinement are listed in Table 1. The final structure formula obtained, $Ta_{14}Si_4(Si_xB_{1-x})_4$ [≡ $Ta_7Si_2(Si_xB_{1-x})_2$ for x = 0.12], yields the composition $Ta_{63.64}Si_{20.36}B_{16}$ (in atom %), differing only slightly from the EPMA value $Ta_{63.6}Si_{18.5}B_{17.9}$ (in atom %) considering the general difficulties in quantitative EPMA of alloys containing Ta and Si as well as the light B element. For each independent crystallographic site, the corresponding coordination polyhedron was derived employing interatomic distances as a criterion combined with an analysis of the Voronoi cell using program DIDO95[15] rejecting (i) neighboring atoms with a Dirichlet area less than 10% of the largest face in a coordination unit and/or (ii) distances d_{Ta-Ta} > 0.33 nm. Coordination polyhedra around Ta atoms exhibit 14, 15, or 16 vertices (CN) (Figure 1 and Table 1) at interatomic distances that range within 0.28 nm < d_{Ta-Ta} < 0.33 nm and are consistent with the radius for Ta atoms (r_{Ta} = 0.146 nm[20]). Silicon atoms are found at the centers of Archimedian antiprisms, the square faces of which are capped by either a Ta3 or a Si atom.

As typical for boron-poor transition metal borides,[21] we encounter the B/Si atoms within a three-capped triangular prism with only one Si/B−Si/B contact at $d_{Si/B-Si/B}$ = 0.2104 nm. Although the site is predominantly filled by boron atoms (88%), the larger radius of Si determines the average distance (taking the radii from Teatum et al.[20] as r_B = 0.088 nm and r_{Si} = 0.134 nm).

X-ray powder diffraction intensities collected from the polycrystalline alloy with nominal composition $Ta_{64.0}Si_{20.0}B_{16.0}$ are in fine agreement with the intensities calculated from the structural model taken from the single crystal. Figure 2 shows the Rietveld evaluation, which converges to R_F = 0.0366 for the main phase $Ta_7Si_2(Si_xB_{1-x})_2$ but also reveals two secondary phases (see Results and Discussion section 3.4). A search for

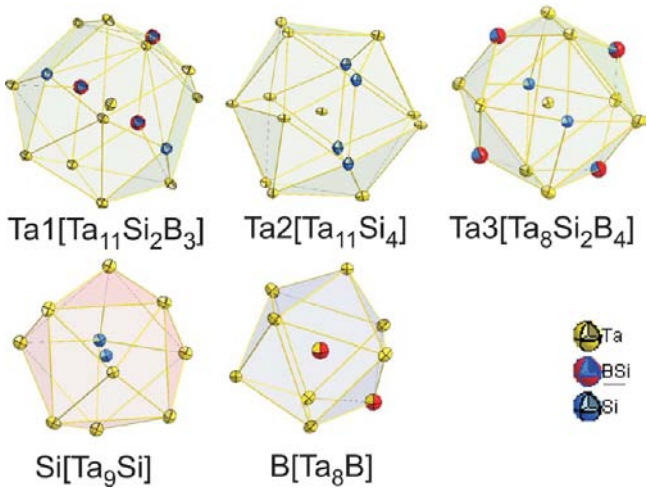

Figure 1. Coordination polyhedra for the independent crystallographic sites in $Ta_7Si_2(Si_xB_{1-x})_2$. Atoms are presented with ADPs from single-crystal refinement (Ta atoms are yellow, Si atoms are blue, and isotropic Si/B atoms (simply labeled as B) are red).

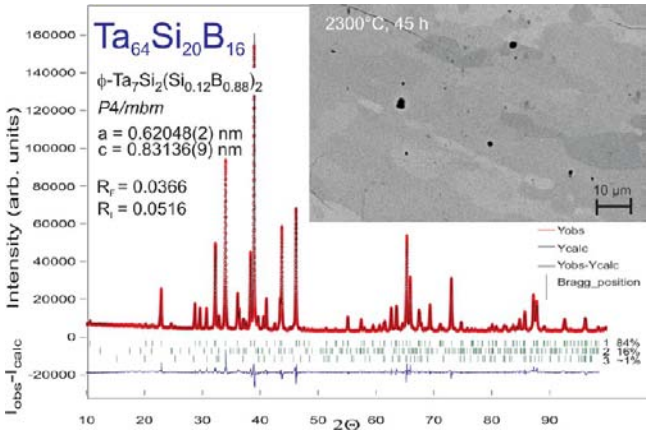

Figure 2. Rietveld refinement of X-ray powder intensity data for alloy $Ta_{64}Si_{20}B_{16}$ annealed at 2300 °C for 45 h. The inset shows a micrograph of the annealed alloy with contrast mainly attributed to crystallographic grain-orientation effects. The main phase (row 1 of hkl labels; 84%) corresponds to $Ta_7Si_2(Si_{0.12}B_{0.88})_2$, row 2 represents the phase $Ta_3(Si_{0.89}B_{0.11})$ (16%), and row 3 stands for the phase $Ta_5(Si_{0.43}B_{0.57})$ (~1%).

the structure type in Pearson's Crystal Data[22] and in ICSD,[23] checking also the Wyckoff sequence $khgea$, prompted a boride structure $(Re,Co)_7B_4$[24] that after standardization reveals isotypism with the structure of $Ta_7Si_2(Si_xB_{1-x})_2$: $Re_4(Re_{0.5}Co_{0.5})_2CoB_2B_2$ ≡ $Ta_4Ta_2TaSi_2(Si_{0.12}B_{0.88})_2$.

3.2. Structural Chemistry of $Ta_7Si_2(Si_xB_{1-x})_2$ (x = 0.12). Structural chemistry of transition-metal borides and silicides is still best described as a function of the metal coordination around the nonmetal atoms (for a detailed description of metal-rich borides, see ref 21). For $Ta_7Si_2(Si_xB_{1-x})_2$, the nearest system-inherent phases are the high-temperature compounds Ta_2B and Ta_2Si, which both crystallize with the $CuAl_2$-type (space group $I4/mcm$) but interestingly do not form any sizable solid solution phase. The typical structural unit in these compounds is the Archimedian antiprism, forming infinite strings along the c axis connected via their square faces. These antiprisms are either centered by a boron atom (with rather long B−B distances at d_{B-B} = 0.2433 nm considered as nonbonding[25]) or by

dx.doi.org/10.1021/ic401413f | Inorg. Chem. 2013, 52, 11295−11301

a Si atom (forming Si−Si contacts at d_{Si-Si} = 0.2528 nm[26]). Although the U_3Si_2-type (space group *P4/mbm*) is a structure type adopted by many transition-metal silicides, Ta_3B_2 rather than Ta_3Si_2 is found to crystallize with this type.[22] The typical structural feature of Ta_3B_2 is a three-capped triangular prism centered by a B atom: B[Ta_{6+2}B]. The B,Si atom in $Ta_7Si_2(Si_xB_{1-x})_2$ forms a loose contact to the one capping B,Si atom at $d_{B,Si-B,Si}$ = 0.2014 nm when compared to the sum of the radii ($2r_B$ = 0.176 nm, $2r_{Si(metal)}$ = 0.268 nm, and $2r_{Si(covalent)}$ = 0.234 nm[20]).

As seen from Figure 3, the structure of $Ta_7Si_2(Si_xB_{1-x})_2$ consists of two characteristic structural elements (see the coordination

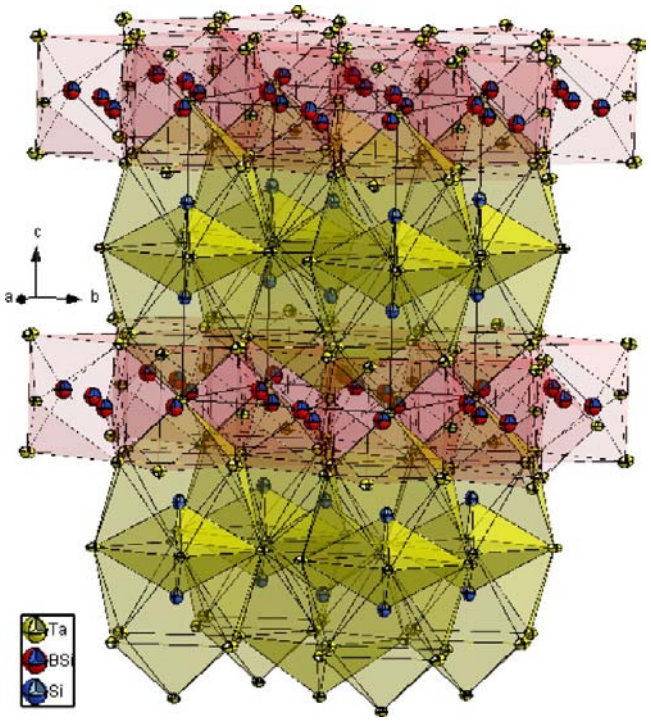

Figure 3. Crystal structure of $Ta_7Si_2(Si_xB_{1-x})_2$ in 3D view revealing layers of three-capped triangular prisms (around Si/B atoms) alternating with layers of Archimedian antiprisms (around Si atoms). Atoms are presented with ADPs from single crystal refinement (Ta atoms are yellow, Si atoms are blue, and isotropic Si/B atoms (simply labeled as B) are red).

polyhedra in Figure 1): (i) a bicapped Archimedian antiprism centered by a Si atom and capped by one Si and one Ta atom, Si[Ta_{8+1}Si], and (ii) a three-capped triangular prism centered by a B/Si-atom, (B,Si)[Ta_{6+2}(B,Si)], where one of the rectangular faces is capped by one B/Si atom. The architecture of the structure of $Ta_7Si_2(Si_xB_{1-x})_2$ combines layers of these triangular prisms (B,Si)[Ta_{6+2}(B,Si)] alternating with double layers of Si[Ta_{8+1}Si] Archimedian antiprisms (Figure 3). Comparing unit cell dimensions and atom site occupation, we see that $Ta_7Si_2(Si_xB_{1-x})_2$ is the first representative of the $(Re,Co)_7B_4$-type,[24] which was described as a member of the homologous structure series $R_{2m+3n}X_{m+2n}$ composing all of the structure types that are close to $Ta_7Si_2(Si_xB_{1-x})_2$ in the Ta−Si−B phase diagram: Cr_5B_3-type ($Ta_5(Si,B)_3$, m = 1, n = 1), $CuAl_2$-type (Ta_2B and Ta_2Si, m = 1, n = 0), and U_3Si_2-type (Ta_3B_2, m = 0, n = 1). Although the B−B contacts in the $(Re,Co)_7B_4$-type[24] were reported to be rather long for bonding contacts (d_{B-B} = 0.194 and 0.220 nm), the larger Si(B) atoms in $Ta_7Si_2(Si_xB_{1-x})_2$ engage in strong contacts $d_{B,Si-B,Si}$ = 0.210 nm and d_{Si-Si} = 0.263 (Results and Discussion section 3.3 below). The site preference observed for the boron atom in $Ta_7Si_2(Si_xB_{1-x})_2$ is perfectly in line with the generally fully ordered transition-metal silico-boride parent structures such as Ti_6Si_2B[28] (K_2UF_6-type), $Ta_5(Si_{1-x}B_x)_3$[10] (Cr_5B_3-type), $Nb_5Si_3B_{1-x}$[10] (Ti_5Ga_4-type), $Co_{4.7}Si_2B$[29] (Nb_5Sn_2Si-type), or Mo_5SiB_2[30] (Mo_5SiB_2-type).

3.3. Electronic Structure Calculations. To introduce the statistical mixture of B and Si in the M1 site, the symmetry of the crystal was reduced to triclinic (space group *P*1), and the unit cell was doubled in the *a* direction (2*a*, *b*, *c*). In the obtained structure, one of the B atoms was substituted by Si, giving $Ta_{28}Si_9B_7$ or $Ta_7Si_2(Si_{0.12}B_{0.88})_2$ to match the experimentally determined composition (EPMA and XRD). The total (for the doubled cell) and partial (for one atom) DOS distribution of $Ta_7Si_2(Si_xB_{1-x})_2$ (x = 0.12) shows (Figure 4) that the d states of the Ta atoms furnish the main contribution to the density of states below the Fermi level. The DOS spectra of Ta1 and Ta2 are rather similar, but both of them differ from Ta3, which appears to have a more localized and sharper distribution of d states near −2 eV.

In all cases, the Ta atoms contribute to both valence and conduction bands. From the DOS spectrum of B (M1 site), it is clear that s and p states overlap (ranging from −7 to −10 eV), yielding s−p hybridization. The distribution of DOS for Si in M1 and Si2 sites shows one prominent feature of the structure: the presence of the partially filled d states in the valence band. These d states could be partially populated via a donor−acceptor mechanism by the formation of π bonds (e.g., Si−O, Si−F, and Si−Cl bonds) with Ta. The effect of s−p hybridization on the Si2 atoms appears to be smaller than on Si in the M1 site and could be explained by the difference in the coordination environment of these types of atoms. Consequently, the density of states profile (s and p states) of Si and B atoms, which share one M1 site, appears to be similar. The total density of states predicts metallic-like behavior of the investigated compound. To understand better the chemical bonding in $Ta_7Si_2(Si_xB_{1-x})_2$, a calculation of the electron localization function was performed (Figure 5). The highest electron localization is observed between the B1−B1 and B1−Si atoms (Figure 6), and some lower electron localization is observed between the Si2−Si2 atoms (Figure 7). Strong polarization of the electron density toward the B1/Si1 atoms between boron/silicon and tantalum is observed.

A similar situation takes place between the Si2 and Ta1, Ta2, and Ta3 atoms. Such features represent $Ta_7Si_2(Si_xB_{1-x})_2$ as a covalent−ionic compound for which the ionic part can be explained on the basis of the difference in electronegativity between the B/Si and Ta atoms. In general, the coordination polyhedra for the B1/Si1 and Si2 atoms represent the bonding picture in the investigated compound. It should be noted that the electron localization maxima between B−B atoms were also observed in the compound $TmAlB_4$,[31] confirming direct (covalent) bonding. This covalent bonding behavior is reflected in the high hardness value presented by the ϕ phase, on the order of 1750 ± 100 HV (≡17.2 GPa), which is an intermediate between the values for Ta silicides such as $TaSi_2$ (1407 HV[32]) and Ta_5Si_3 (1200−1500 HV[32]) as well as the Ta boride Ta_3B_2 (2770 HV[32]) within the homologous structure series $R_{2m+3n}X_{m+2n}$.

Taking at the Fermi level 3.21 states/eV for 1 formula unit (note that Figure 4 shows 12.86 states/eV at E_F for the doubled cell with 44 atoms), we can extract the Sommerfeld constant,

dx.doi.org/10.1021/ic401413f | *Inorg. Chem.* 2013, 52, 11295−11301

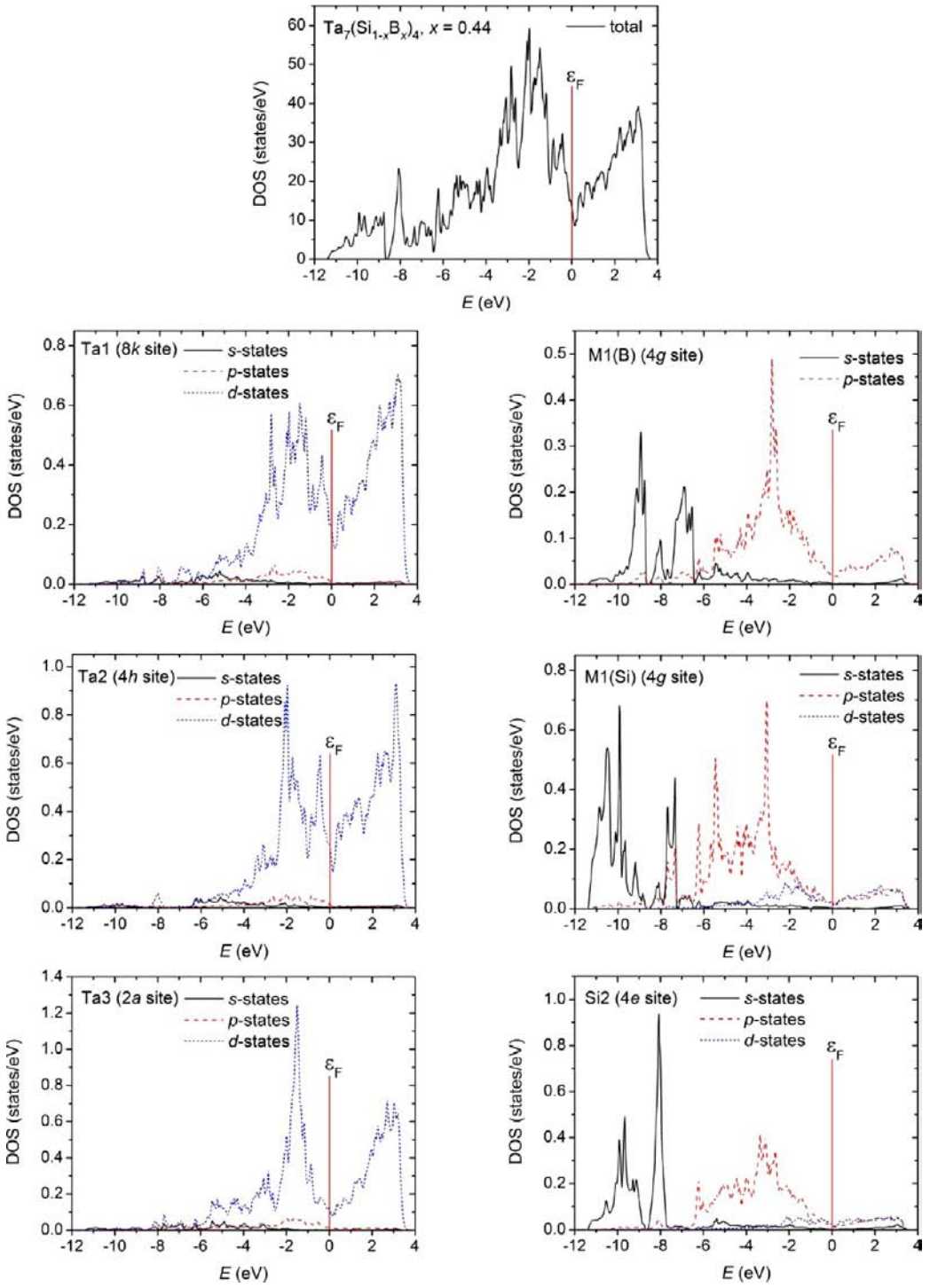

Figure 4. Distribution of the total (for the doubled cell in the *a* direction) and partial (for one atom) density of states in $Ta_7Si_2(Si_xB_{1-x})_2$ ($x = 0.12$) (Fermi level at $E = 0$).

$\gamma = 7.58$ mJ/molK^2, which suggests typical metallic behavior for $Ta_7Si_2(Si_xB_{1-x})_2$.

3.4. $Ta_7Si_2(Si_xB_{1-x})_2$ and Phase Diagram. The composition of the new phase $Ta_7Si_2(Si_xB_{1-x})_2$, as refined from the single-crystal study, is close to the composition of the so-called ϕ phase (which earlier was tentatively located at the composition $Ta_2(Si_{0.54}B_{0.46})$[8] in the isothermal section of the Ta−Si−B system at 1900 °C). It has been proposed that at 1900 °C this ϕ phase equilibrates with Ta_{ss} (ss = solid solution), $Ta_3(Si_{1-x}B_x)$, $Ta_5(Si_{1-x}B_x)_3$ [Cr_5B_3-prototype], and $Ta_2(Si_{1-x}B_x)$.[8] The phase relations derived for the partial isothermal section at 2000 °C, as shown in Figure 8, are close to those presented earlier at 1900 °C.[8] As the X-ray intensity pattern of the ϕ phase appeared most intense in the alloy $Ta_{64}Si_{20}B_{16}$, from which the single crystal was extracted and a quantitative Rietveld refinement confirmed the new phase, there is no doubt about the identity between the ϕ phase[8] and $Ta_7Si_2(Si_xB_{1-x})_2$.

Although the crystal structure of $Ta_7Si_2(Si_xB_{1-x})_2$ contains one crystallographic site with a random mixture of B and Si atoms, no homogeneous region has so far been experimentally

dx.doi.org/10.1021/ic401413f | Inorg. Chem. 2013, 52, 11295−11301

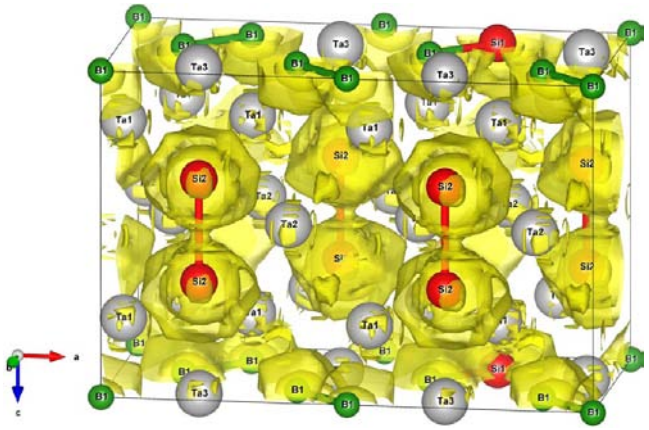

Figure 5. Electron localization at 0.55 in $Ta_7Si_2(Si_xB_{1-x})_2$ (x = 0.12). The unit cell is doubled in the a direction.

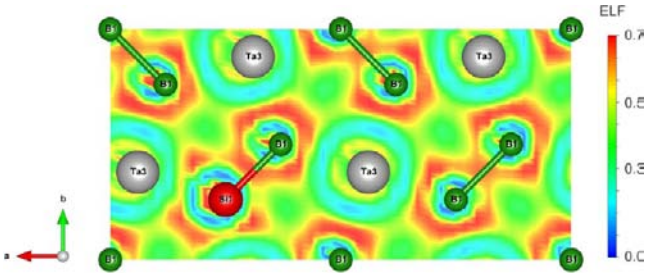

Figure 6. Projection of the electron localization distribution on the (001) lattice plane in $Ta_7Si_2(Si_xB_{1-x})_2$ (x = 0.12).

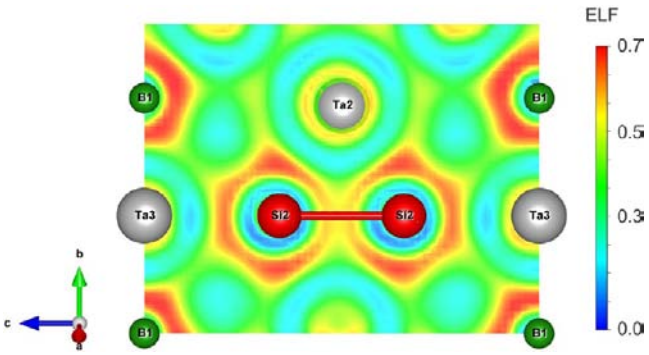

Figure 7. Projection of the electron localization distribution on the (100) lattice plane formed by B1–Si2–Ta3 atoms in $Ta_7Si_2(Si_xB_{1-x})_2$ (x = 0.12).

encountered for the phase ϕ. The Rietveld refinement of the X-ray powder intensity data for alloy $Ta_{64}Si_{20}B_{16}$ (annealed at 2300 °C; Figure 2) revealed two phases besides the main phase of $Ta_7Si_2(Si_xB_{1-x})_2$, namely, $Ta_3(Si_{1-x}B_x)$ with Ti_3P-type (about 16% of the total intensity spectrum) and traces of the T2 phase, $Ta_5(Si_{1-x}B_x)_3$ with the Cr_5B_3-type (~1%).

Although the sensitivity in atom site occupation is limited for a secondary phase at reduced amounts, we observe good agreement for the B content in the Ti_3P-type phase (x = 0.11; i.e., ~3 atom % B) with the experimental data (~3 atom % B in Ta_3Si) derived from the phase diagram at 2000 °C (Figure 8). The traces of the T2 phase ($Ta_5(Si_{1-x}B_x)_3$ with the Cr_5B_3-type (~1%), however, do not allow any reliable determination of the B content and with lack of reliable EPMA data from the microstructure, the composition data were introduced from our

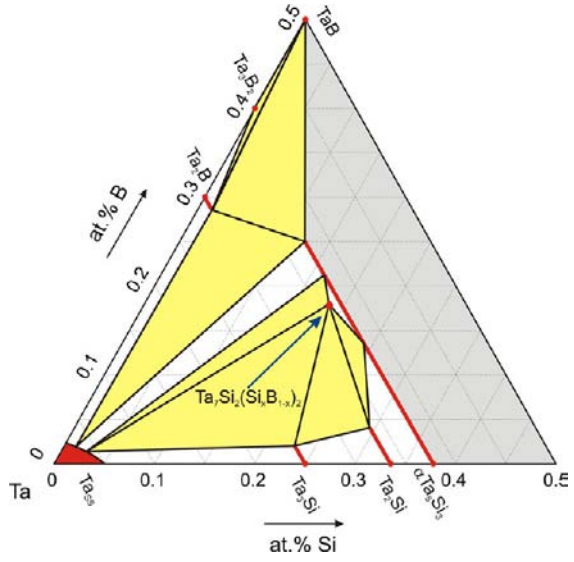

Figure 8. Partial isothermal section at 2000 °C for the Ta-rich part of the Ta–Si–B system.

single-crystal study of $Ta_5(Si_{0.43}B_{0.57})_3$.[10] It should be noted, however, that the Rietveld refinement of alloy $Ta_{64}Si_{20}B_{16}$ (Figure 2) with main and secondary phases clearly defines the tie-line $Ta_7Si_2(Si_xB_{1-x})_2$ (x = 0.12) + $Ta_3(Si_{1-x}B_x)$ (x = 0.11), which is in agreement with the phase triangulations at 1900 °C[8] as well as at 2000 °C (ϕ phase + $Ta_3(Si_{1-x}B_x)$). The composition of the ϕ phase ($Ta_2(Si_{0.54}B_{0.46})$), as determined from the phase triangulation at 1900 °C,[8] differs by a small but significant amount from $Ta_7Si_2(Si_{0.12}B_{0.88})_2$, as obtained from the present single-crystal X-ray analysis in close correspondence to the EPMA analysis of $Ta_{63.6}Si_{18.5}B_{17.9}$ for the ϕ phase in the isothermal section at 2000 °C. Although the ratio Ta/nonmetals is different, it is worth noting that the single-crystal refinement without constraints converged to a Si/B ratio identical with the EPMA experiment. From the ADPs derived in the single-crystal study, we see quite uniform values for all Ta sites and the Si2 site. In addition, the slightly higher ADP value for the Si/B site, which is dominated by the light B atom, is well conceivable. With the experimental difficulties in arriving at reliable EPMA data for the light atoms near heavy Ta, Si defects in the Si/B site can neither be introduced into the refinement nor can reliable quantitative X-ray refinements be obtained from three species in one crystallographic site (B, Si, and a vacancy).

4. CONCLUSIONS

The crystal structure of a new refractory boron silicide, $Ta_7Si_2(Si_xB_{1-x})_2$ (x = 0.12), was determined from X-ray single crystal (XSC) and powder diffraction data (XPD). Tetragonal $Ta_7Si_2(Si_xB_{1-x})_2$ (space group $P4/mbm$; a = 0.62219(2) nm and c = 0.83283(3) nm) with B atoms randomly sharing the 4g site with Si atoms is isotypic with the boride structure of $(Re,Co)_7B_4$. The architecture of the structure of $Ta_7(Si_{1-x}B_x)_4$, combining layers of three-capped triangular metal prisms (B,Si)[Ta_{6+2}(B,Si)] alternating with double layers of two-capped Si[Ta_{8+1}Si] Archimedian metal antiprisms, is typical for metal borides of low boron content. Consequently, the two types of coordination figures around the nonmetal atoms are inherent to the structures of Ta_2B (or Ta_2Si) and Ta_3B_2.

Partial substitution of B by Si atoms does not significantly change the bonding picture in the structure. Strong electron density localization between B–B(Si) and Si–Si atom pairs

dx.doi.org/10.1021/ic401413f | Inorg. Chem. 2013, 52, 11295–11301

confirms covalent bonding and represent $Ta_7Si_2(Si_xB_{1-x})_2$ as a covalent−ionic compound of high hardness (1750 HV). Typical metallic behavior is inferred from the Sommerfeld constant, γ = 7.58 mJ/mol K^2, as derived from the electronic density of states at the Fermi level.

■ ASSOCIATED CONTENT

Supporting Information

Crystallographic data in CIF format. This material is available free of charge via the Internet at http://pubs.acs.org.

■ AUTHOR INFORMATION

Corresponding Author

*Tel: +43-1-4277-52456; Fax: +43-1-4277-9524; E-mail: peter.franz.rogl@univie.ac.at.

Notes

The authors declare no competing financial interest.

[#]On leave of absence from Lviv Polytechnic National University, Ukraine

■ ACKNOWLEDGMENTS

The authors acknowledge FAPESP (São Paulo, Brazil), grant 99/09327-3, for financial support. Part of this research was supported by the European Commission under the 6th Framework program through the Key Action: Strengthening the European Research Area, Research Infrastructures (contract no. RII3-CT-2003-505925).

■ REFERENCES

(1) Lemberg, J. A; Ritchie, R. O. *Adv. Mater.* **2012**, *24*, 3445−3480.
(2) Thom, A. J.; Summers, E.; Akinc, M. *Intermetallics* **2002**, *10*, 555−570.
(3) Parthasarathy, T. A.; Mendiratta, M. G.; Dimiduk, D. M. *Acta Mater.* **2002**, *50*, 1857−1868.
(4) Suzuki, H.; Kitani, K.; Iwase, H.; Makoto, K. *Jpn. Kokai Tokkyo Koho Patent* JP 2008213374 A, September 18, 2008.
(5) Nowotny, H.; Lux, B.; Kudielka, H. *Monatsh. Chem.* **1956**, *87*, 447−470.
(6) Kudielka, H.; Nowotny, H.; Findeisen, G. *Monatsh. Chem.* **1957**, *88*, 1048−1055.
(7) Guo, Z.; Yuan, W.; Sun, Y.; Cai, Z.; Qiao, Z. *J. Phase Equilib. Diffus.* **2009**, *30*, 564−571.
(8) Ramos, E. C. T.; Nunes, C. A.; Coelho, G. C. Technical Report from the 57th Congresso Anual, Associacao Brasileira de Metalurgia e Materiais: Sao Paulo, Brazil, July 2002; pp 359−368 (in Portuguese).
(9) Ramos, A. S.; Ramos, E. C. T.; Neto, C. M. *Mater. Sci. Forum* **2006**, *530−531*, 197−202.
(10) Khan, A. U.; Nunes, C. A.; Coelho, G. C.; Suzuki, P. A.; Grytsiv, A.; Bourreé, F.; Giester, G.; Rogl, P. F. *J. Solid State Chem.* **2012**, *190*, 1−7.
(11) Roisnel, T.; Rodriguez-Carvajal, J. *Mater. Sci. Forum* **2001**, *118*, 378−381.
(12) *INCA Energy 300*; Oxford Instruments Analytical Ltd.: Oxford, U.K., 2000.
(13) *Nonius Kappa CCD, Program Package: COLLECT, DENZO, SCALEPACK, SORTAV*; Nonius Delft: The Netherlands, 1998.
(14) Sheldrick, G. M. *SHELXL-97, A Program for Crystal Structure Refinement*; University of Göttingen: Göttingen, Germany, 1997.
(15) Koch, E.; Fischer, W. *Z. Kristallogr.* **1996**, *211*, 251−253.
(16) *ELK, DFT Program Package*; University of Graz: Graz, Austria; http://elk.sourceforge.net/.
(17) Perdew, J. P.; Burke, K.; Ernzerhof, M. *Phys. Rev. Lett.* **1996**, *77*, 3865−3868.
(18) Momma, K.; Izumi, F. *J. Appl. Crystallogr.* **2008**, *41*, 653−658.
(19) Farrugia, L. J. *J. Appl. Crystallogr.* **1999**, *32*, 837−838.
(20) Teatum, E.; Gschneidner, K.; Waber, J. *Report No. LA-2345*; U.S. Department of Commerce: Washington, DC, 1960.
(21) Rogl, P. Formation of Borides. In *Inorganic Reactions and Methods: Formation of Bonds to Group-I, -II, and -IIIB Elements*; Zuckerman, J. J., Hagen, A. P., Eds.; John Wiley & Sons, Inc.: Hoboken, NJ, 1991; Vol. *13*.
(22) Villars, P.; Cenzual, K. *Pearson's Crystal Data: Crystal Structure Database for Inorganic Compounds*; ASM International: Materials Park, OH [CD-ROM] 2012−2013.
(23) *ICS database 2012/1*: Fachinformationszentrum: Karlsruhe, Germany.
(24) Krypyakevich, P. I.; Kuzma, Yu. B.; Chepiga, M. V. *Dopov. Akad. Nauk Ukr. RSR, Ser. A* **1972**, *9*, 856−858.
(25) Rudy, E.; Benesovsky, F.; Toth, L. Z. *Z. Metallkde.* **1963**, *54*, 345−352.
(26) Havinga, E. E.; Damsma, H.; Hokkeling, P. J. *J. Alloys Compd.* **1972**, *27*, 169−178.
(27) (a) Gelato, L. M.; Parthé, E. J. *Appl. Crystallogr.* **1987**, *20*, 139−143. (b) Parthé, E.; Gelato, L.; Chabot, B.; Penzo, M.; Censual, K.; Gladyshevskii, R. *TYPIX. Standardized Data and Crystal Chemical Characterization of Inorganic Structure Types*; Springer-Verlag: New York, 1994.
(28) Ramos, A. S.; Nunes, C. A.; Rodrigues, G.; Suzuki, P. A.; Carvalho Coelho, G.; Grytsiv, A. V.; Rogl, P. *Intermetallics* **2004**, *12*, 487−491.
(29) Åronsson, B.; Lundgren, G. *Acta Chem. Scand.* **1959**, *13*, 433−441.
(30) Åronsson, B. *Acta Chem. Scand.* **1958**, *12*, 31−37.
(31) Mori, T.; Borrmann, H.; Okada, S.; Kudou, K.; Leithe-Jasper, A.; Burkhardt, U.; Grin, Yu. *Phys. Rev. B* **2007**, *76*, 064404-1−064404-10.
(32) Samsonov, G. V.; Vinitskii, I. M. *Handbook of Refractory Compounds*; IFI/Plenum: New York, 1980.